Optical switching using fiber ring reflectors

J. D. Moores, K. Bergman, H. A. Haus, and E. P. Ippen

Department of Electrical Engineering and Computer Science and Research Laboratory of Electronics, Massachusetts Institute of Technology, Cambridge, Massachusetts, 02139

Received December 29, 1989; accepted August 16, 1990

We present the results of studies of fiber ring reflectors that are pulse excited in the negative dispersion regime. An intensity-dependent fiber switch is proposed for improved thresholding and pulse output characteristics over those previously reported. Schemes for fiber switches relying on solitary-wave collision-induced phase shifts are also discussed. A pulse regenerator and logic gates are proposed, each capable of correcting timing drifts.

INTRODUCTION

Interferometric all-optical pulse interaction systems have a long history of proposals and experiments. An interferometric logic gate using a Mach–Zehnder waveguide interferometer was proposed and its nonlinear response tested.[1] Stable interference is achieved with an interferometer in a ring configuration, as was realized by Otsuka, who proposed the ring as an optical logic device.[2] The virtue of the ring configuration is that the interference is insensitive to changes in the linear index of the interferometer owing to temperature changes and other environmental effects. Doran *et al.*[3] published data on a nonlinear fiber ring interferometer, operating in the positive dispersion regime, in which the coupler ratio was 58/42. In this arrangement, the two countertraveling pulses accumulated different nonlinear phase shifts that were a function of the input intensity. Theoretical curves were shown of output-versus-input pulse energy along with experimental confirmation.

When the ring interferometer is operated in the positive dispersion regime, self-phase modulation leads to a nonuniform phase across the pulse, and it is to be expected that the shape of the output pulses would be thereby affected. We performed experiments in this regime on a 25-m Sagnac loop with an 85/15 input coupler ratio. The experiments clearly showed that the nonuniform phase produces output pulses of a complicated structure. Figure 1 gives comparisons between the predicted and observed autocorrelation traces of the reflected pulses. In anticipation of such effects, Doran and Wood[4] suggested operation in the negative dispersion regime using solitons. Of course, the uneven division of energy between the two counterpropagating pulses does not produce perfect solitons. However, operation of the device is helped by the fact that the pulses tend to adjust themselves toward solitons if the propagation distance is several soliton periods. Yet even then, when the pulses interfere at the coupler to produce an output, their widths are not equal, and imperfect output pulse profiles result.

Experiments employing the imbalanced Sagnac interferometer in the negative dispersion regime were performed by Blow *et al.*[5] and Islam *et al.*[6] Blow *et al.*[5] used a 58/42 ratio coupler and 100 m of fiber, obtaining a maximum throughput of 93% and a minimum linear transmission of 2.56%. In the experiment reported by Islam *et al.*,[6] a 68/32 ratio coupler and 25 m of fiber were used to attain switching from a 12.96% linear transmission to 90% transmission at the first output energy peak. The degree of coupler imbalance establishes a lower bound on the switching curve but also dictates the length of fiber required to achieve a relative phase of π.

In this paper we propose a design of a ring reflector with a 50/50 coupler ratio that operates as an improved switch. It has the advantage that, unlike in the results of Blow *et al.*[5] and Islam *et al.*,[6] small input pulses produce essentially zero output. The nonlinear imbalancing of the ring interferometer is accomplished by alternation of the principal propagation axes along the birefringent fiber. The fiber loop is arranged such that one pulse remains polarized along a principal axis but the counterpropagating pulse is polarized at 45° to the axis. The counterpropagating pulse thus splits into two orthogonal, smaller pulses, which travel along the principal axes and recombine only after traversing the loop length.

In a modified form the ring reflector can perform as a pulse regenerator or a logic gate. Through computer studies we have found that when two orthogonally polarized solitary waves interact on a highly birefringent fiber, they do not change each other's shape significantly if the exchanged phase shift is small compared with π. Thus we are led to propose a second switching mechanism that utilizes this concept, whereby a control pulse slides through the signal pulse several times until the signal pulse accumulates a total of π phase shift.

COMPUTER MODEL

The coupled nonlinear Schrödinger equations (CNSE's) are used to model pulse propagation in a birefringent fiber. With appropriate normalizations, the CNSE's take the form

$$-iu_x = \tfrac{1}{2}u_{tt} + (|u|^2 + \alpha|v|^2)u,$$

$$-i(v_x - \sigma v_t) = \tfrac{1}{2}v_{tt} + (|v|^2 + \alpha|u|^2)v,$$

where u and v are the orthogonally polarized complex fields, the subscripts indicate derivatives with respect to

0740-3224/91/030594-08$05.00

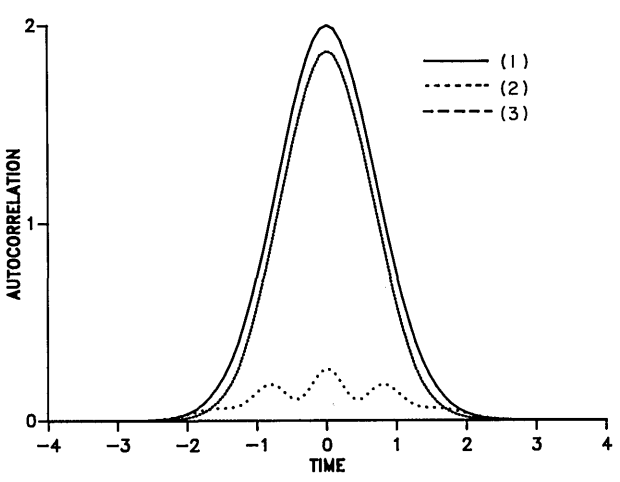

(a)

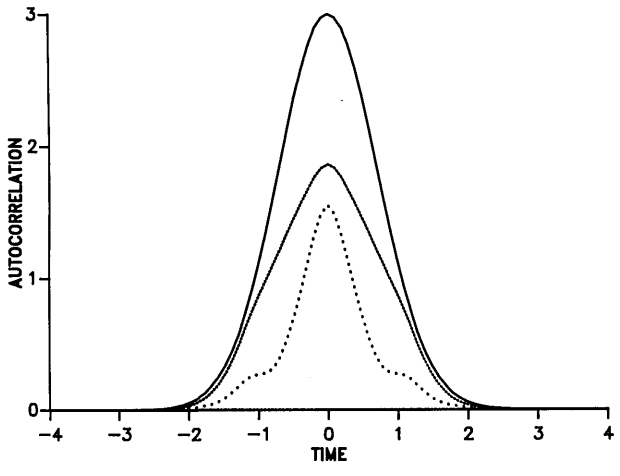

(b)

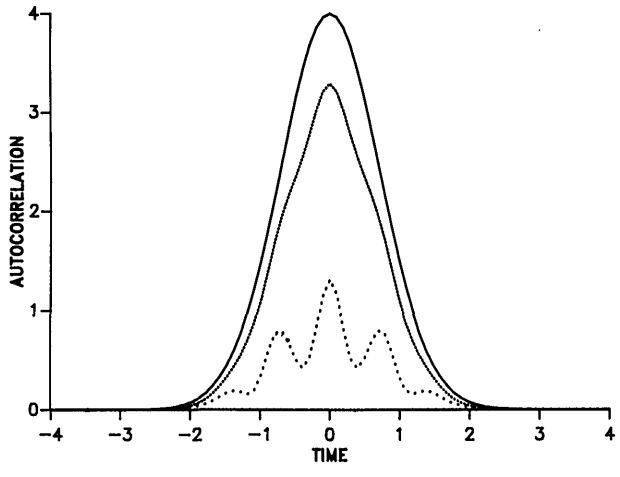

(c)

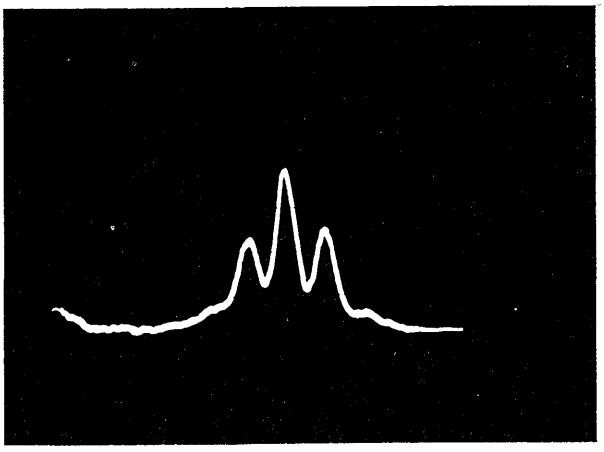

(d)

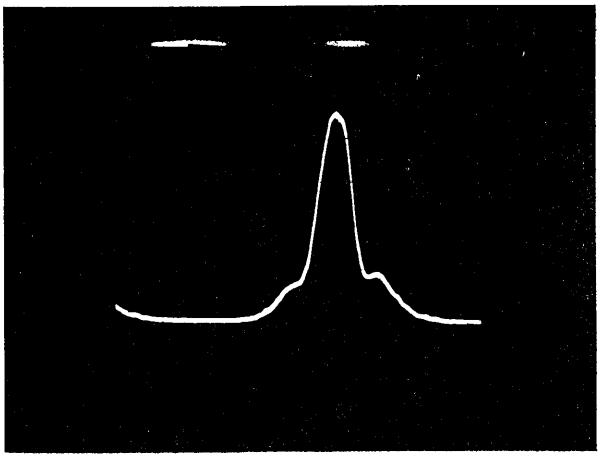

(e)

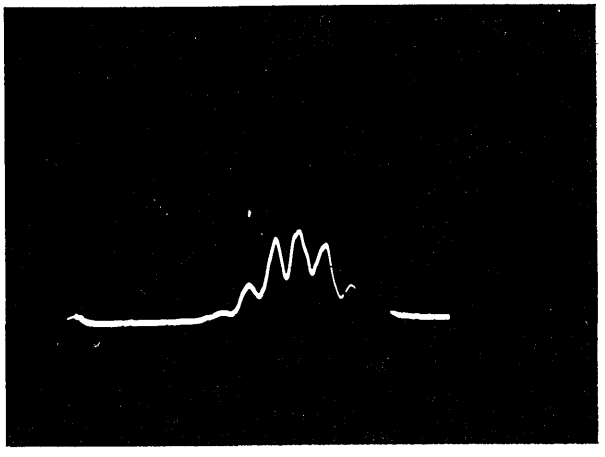

(f)

Fig. 1. Computed and experimental autocorrelations in the positive dispersion regime. The theoretical plots [(a)–(c)] show the input pulse (1), the transmitted pulse (2), and the reflected pulse (3). Only the reflected pulse experimental autocorrelations are shown [(d)–(f)].

the spatial and temporal variables x and t, and α is the cross-phase coupling coefficient (2/3 for linear polarization). The coordinate frame is selected such that the u pulse, in the absence of the v pulse, is stationary. The normalized group-velocity difference of the u and v pulses appears as σ, which we call the slip:

$$\sigma = 2\pi\Delta n(0.5673\tau)/(\lambda^2 D), \quad (1)$$

where Δn is the birefringence, τ is the pulse width, λ is the wavelength, and D is the dispersion (psec nm^{-1} km^{-1}).

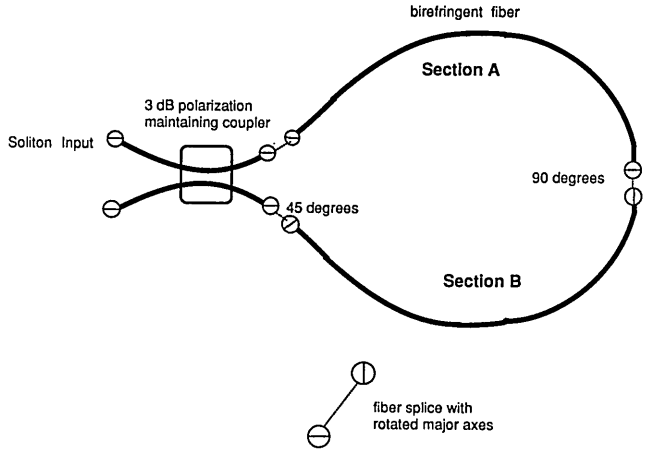

Fig. 2. Proposed fiber loop intensity switch with rotated birefringence axes.

Throughout this paper, it is assumed that counterpropagating pulses interact negligibly. For details of the other normalizations, the reader is referred to Ref. 7.

For linear polarization, the CNSE's contain additional cross-coupling terms, or coherence terms, which are significant in the low-birefringence (small-slip) limit. For our purposes, the coherence terms can be ignored as long as the beat length is much shorter than the soliton period. This condition is satisfied in all of the simulations discussed in this paper.

Note that the noninstantaneous response of the fiber is not accounted for in this model. With subpicosecond pulses, the associated self-frequency shift becomes nonnegligible. This issue is addressed by Islam *et al.*,[6] who conclude that for their fiber switch the effect is significant when higher-order solitonlike pulses are involved, i.e., at energies higher than the intended operating range of the device. Our switch involves longer pulses, shorter fiber lengths, and a fiber with half the response time (we assumed silica fiber). Each of these changed parameters lessens the expected self-frequency shift. The other class of devices discussed in this paper, solitary-wave collisional gates, can be designed to be unaffected by self-Raman-induced time shifts.

We employ a simple finite-difference scheme in time, using a seven-point approximation for the second-order temporal derivatives. In space, we leapfrog.[8] Hard boundary conditions are imposed at the edges of our temporal windows; i.e., the fields are forced to zero. We avoid reflection problems by selecting sufficiently large temporal windows. The optimal size of the window is determined by the degree to which the pulse energy remains localized, and this is clearly a function of the initial conditions.

FIBER INTENSITY-DEPENDENT SWITCH

Figure 2 shows a design of a ring interferometer that uses a 50/50 coupler. The linear response of this ring is such that no output is produced (for sufficiently weak input pulses). In order to achieve a nontrivial nonlinear response, we split the polarization-maintaining fiber into two sections, with the fast and slow axes oriented as indicated. An input pulse is separated by the coupler into two equal pulses of half-intensity. The pulse entering section A follows the fast axis in the first half and the slow axis in the second half. The second pulse enters the fiber through section B, polarized at 45° with respect to the fast axis. It splits into two pulses of different speeds. These two lower-intensity pulses accumulate nonlinear phase shifts at a slower rate than the counterpropagating pulse. In section A the axes are interchanged and the two versions of the pulse recombine. For pulses of the form A sech t (normalized units) in the negative dispersion regime, the nonlinear phase shift is computed by the approximation[9]

$$\phi = \begin{cases} 2(A - \frac{1}{2})^2 z, & A \geq 1/2 \\ 0, & 0 \leq A < 1/2 \end{cases} \quad (2)$$

Figure 3 shows the output pulse energy versus input pulse energy as computed analytically, accompanied by the results of the simulations. In terms of the input pulse intensity,

$$\phi(\text{device}) = z/2[I - (2\sqrt{2} - 2)\sqrt{I}], \quad (3)$$

where ϕ is now the relative nonlinear phase shift for the complete device, I is the input intensity relative to a normalized-unit-width hyperbolic secant pulse, and $z = \pi L(2z_0)$, with L being the physical fiber length and z_0 the soliton period.[10] The first relative nonlinear phase shift of π occurs for

$$z = 2\pi/[I - (2\sqrt{2} - 2)\sqrt{I}]. \quad (4)$$

The length of the device thus determines at which input pulse energy the maximum transmission occurs. We simulated a device whose transmission maximum was three times the $N = 1$ soliton energy, so that the three pulses traveling within the loop were each nearly $N = 1$ solitons. Note that if one were to try to achieve peak transmission at significantly lower than three times the $N = 1$ energy, the nonlinearity would be too weak to inhibit dispersion.

Profiles of the emerging pulse shapes are illustrated in Fig. 4. These computed results were obtained for a

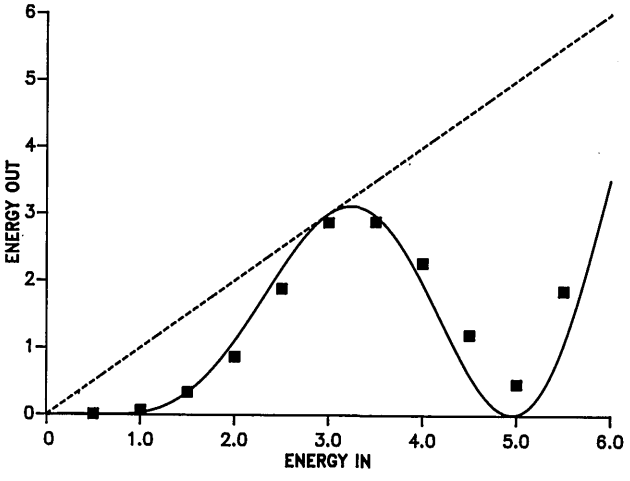

Fig. 3. Output pulse energy versus input pulse energy. The curve is computed from Eqs. (2) and (3). The points are computed from simulations.

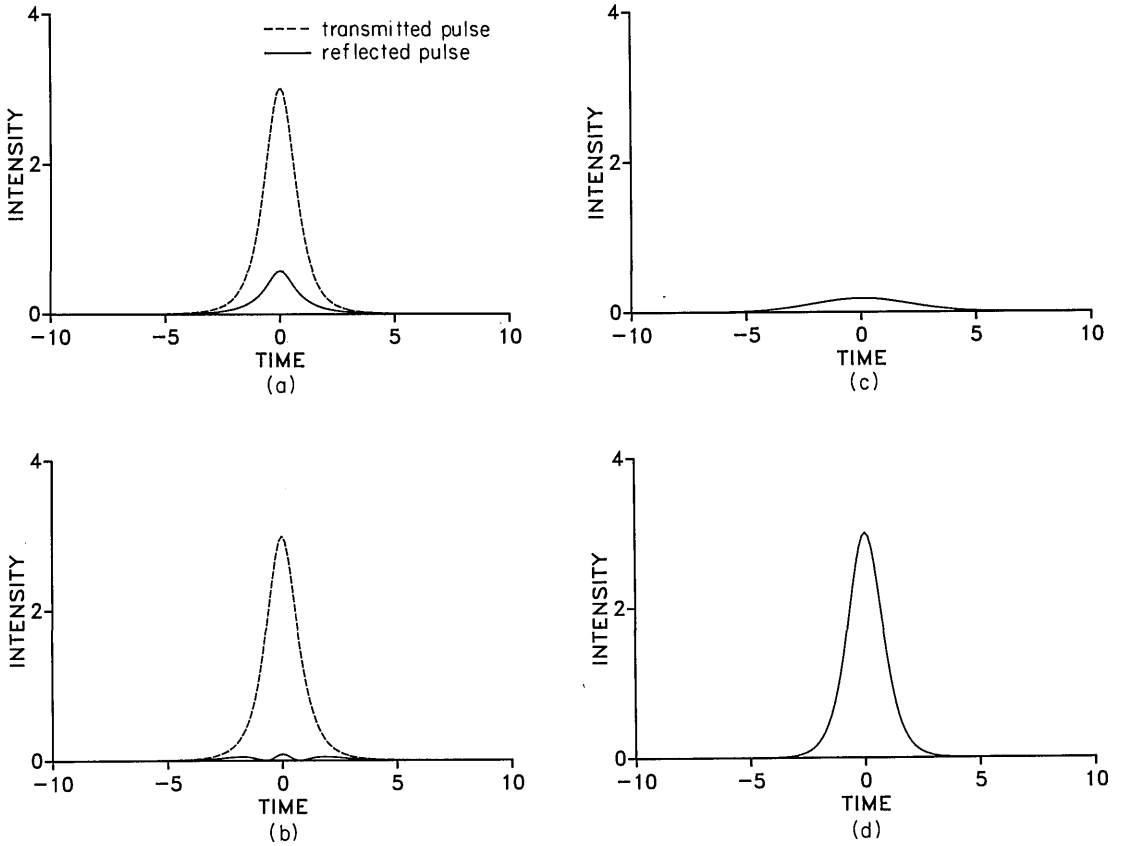

Fig. 4. Transmitted and reflected intensity profiles for normalized input energies of 3.5, 3.0, and 0.5 shown in plots (a), (b), and (c), respectively. The input pulse is shown for comparison (d).

total loop length of 18.3 m with pulse widths of 500 fsec at 1.55 μm. The assumed dispersion was 13.89 psec nm^{-1} km^{-1}, and the birefringence used was $\Delta n = 5.62 \times 10^{-4}$. We opted for a large birefringence in order to ensure that the pulse entering at 45° splits cleanly. The input energy is in normalized units such that unit energy refers to a fundamental soliton of unit amplitude and width. With these parameters the $N = 1$ soliton energy is 31 pJ and its period is 7.1 m.[10] If one were to operate the device at 10 Gbits/sec, the average power would be roughly 1 W. The projected power level is not entirely realistic. However, the main objective of the present proposal is to outline schemes that preserve or even improve the pulse shape and the spectrum of the pulses. Switch designs using the interferometric principle will have to be variations on the theme developed here. Realistic switch designs may still have to await the development of materials with higher nonlinearities.

In our simulation we assumed that the two fiber sections were perfectly matched in length. The pulse entering the fiber polarized at 45° splits along the fast and slow axes in the first section and must be recombined with the correct polarization at the end of the second section. For our birefringence, matching the two pulses to within 1/20 of a wavelength corresponds to matching the lengths of the two sections to within 0.21 mm.

In Fig. 4 we show three sets of reflected and transmitted pulse profiles for input energies of 0.5, 3.0, and 3.5. With the 0.5 input, 99% of the pulse is reflected, while at the curve peak with an input energy of 3.0, 97% of the pulse is transmitted. Even beyond the peak energy, we observe that with an input energy of 3.5, 78% of the energy is transmitted, providing a transmitted pulse close to the 3.0 energy pulse. The output pulse shape shows little distortion.

It should be pointed out that the device does not operate, strictly, with solitons. In the first place, if the pulse along the fast (or slow) axis of the polarization-maintaining fiber is a soliton, the countertraveling pair do not commence as solitons because each has half the intensity. Additionally, the CNSE's describing the propagation of the two orthogonally polarized pulses are not integrable. Yet the orthogonal pulse interaction is small and the overall performance of the device is quite satisfactory.

Next we address the issue of pulse-width preservation. A device with length much less than a soliton period would preserve pulse widths, but in order to obtain sufficient net phase shift we require higher-order solitons. In the example discussed above, the fiber loop length exceeds the soliton period. This implies that the loop length is sufficient for the pulses to reshape within the loop. However, one can take advantage of the area-preserving nature of solitons and employ saturating amplification to restore the desired pulse width.[11]

SOLITARY-WAVE COLLISION DEVICES

The proposed intensity switch described above relies on the difference in nonlinear phase-shift accumulation between pulses of different intensities. We now take advan-

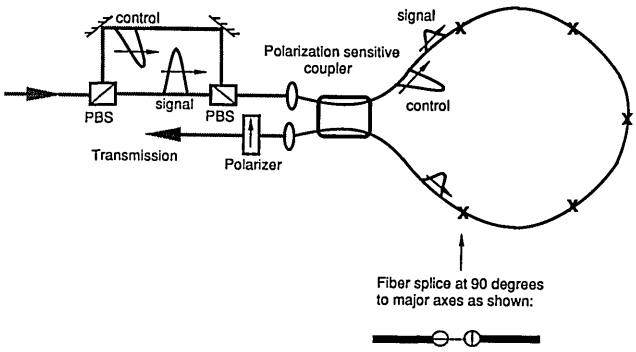

Fig. 5. Proposed simple ring interferometer AND gate employing solitary-wave collisions with birefringent fiber sections (six sections shown). This device can be used as a pulse regenerator. The X's indicate fiber splices. PBS, polarizing beam splitter.

tage of the near integrability of the CNSE's with high birefringence and use gentle solitary-wave collisions to provide the necessary phase shifts. By gentle, we mean that the effect of a collision on a solitonlike pulse is a phase shift and a small temporal displacement but negligible shift in frequency and intensity. Solitonlike describes a pulse that would be a soliton in the absence of coupling to excitations polarized along the orthogonal axis (the uncoupled equations are integrable).

A feature of solitary-wave collisions is the appearance of shadows, for sufficiently small slip. As a result of a collision, each solitary wave may pick up an orthogonally polarized, copropagating shadow. Through our simulations with linearly birefringent fiber, we discovered that for slip greater than 2, the shadows are small compared with the main pulses, for our pulse energies.

As is shown in Fig. 5, the device is again a fiber loop, but we have increased the number of fiber sections within the loop. At each splice, we align the fast axis of one section with the slow axis of the other. No 45° splice is used. The coupler is 50/50 for one polarization (corresponding to the signal pulse) and 100/0 for the other polarization (the control pulse). At the input to the device, the control pulse (fast axis) is delayed with respect to the signal (slow axis). Note that the polarizing beam splitters (PBS's) at the input in Fig. 5 (and in subsequent figures) are shown for conceptual clarity: they may be replaced by fiber components. In the first loop section, the control pulse catches up with the clockwise propagating signal, interacts with the signal, and subsequently passes it. In the second fiber section, the signal catches, interacts with, and passes the control. The process is repeated through the remaining fiber sections.

The birefringence is selected such that the pulses acquire as much phase shift as possible without being significantly displaced or distorted. The collisional phase shift depends only on the effective index seen by a pulse, and clearly this is independent of the parity of the relative speed of the control and the signal. The collisional displacement does depend on the parity of the relative pulse speed and can be thought of as a tendency of one pulse to try to capture the other. Small collisional displacements are tolerable, particularly since the displacements of successive collisions cancel.

The lengths of the individual sections of fiber need not be identical. In fact, they could differ substantially. We require that each section be of sufficient length that the two pulses, separated by at least a pulse width, collide and separate by at least a pulse width on reaching the end of the section. If the slip is sufficiently small, and therefore the interaction sufficiently strong, then it may be necessary to increase the length of each section in order that the pulses equilibrate following each collision.

We obtain excellent results from our simulation when the input pulses are (normalized) unit-width hyperbolic secants with twice the $N = 1$ soliton energy. The device that we discuss contains 14 sections and has a total length of 42.7 m, and the birefringence is $\Delta n = 2.15 \times 10^{-4}$. The accumulated collisional phase shift, acquired by half the input pulse, as a function of distance along the loop, is plotted in Fig. 6. Note that we intentionally selected our fiber length and initial pulse spacings to demonstrate that the collisions need not occur in the centers of the fiber sections. Figure 7(a) shows the control pulse. Figure 7(b) shows the half of the signal pulse that has undergone 14 collisions, before interference at the coupler. As is shown, the signal pulse maintains its shape and accumulates a constant π phase shift. There is a slight asymmetry in the phase, but this is simply due to the nonzero overlap of the pulse tails.

To demonstrate the cleanliness of the output despite noisy, degraded inputs, we sent the control pulse shown in Fig. 7(c) into the device. The noisy pulse was still able to switch the locally generated signal pulse [compare Fig. 7(b) with Fig. 7(d)], and the device replaces the control with the switched signal.

In the configuration depicted in Fig. 5, the control pulse always leaves the device through the transmission port, but the signal is transmitted only in the presence of the control and is reflected in the absence of the control. The device operates as an AND gate with no gain if a polarizer is placed at the transmission port to suppress the control pulse.

The signal pulse and the control pulse function as the two inputs to the device. If only the control pulse is present, no output is produced. The same holds for the signal pulse. An output is produced solely when both are present.

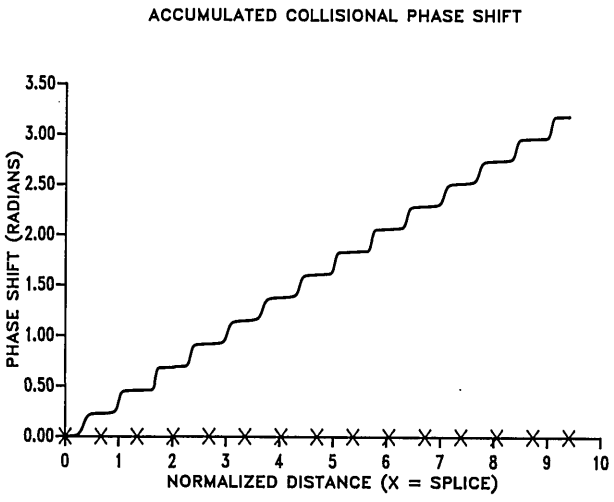

Fig. 6. Phase shift of one pulse, accumulated through 14 solitary-wave collisions, as a function of distance. The phase is in radians. The X's indicate fiber splice locations.

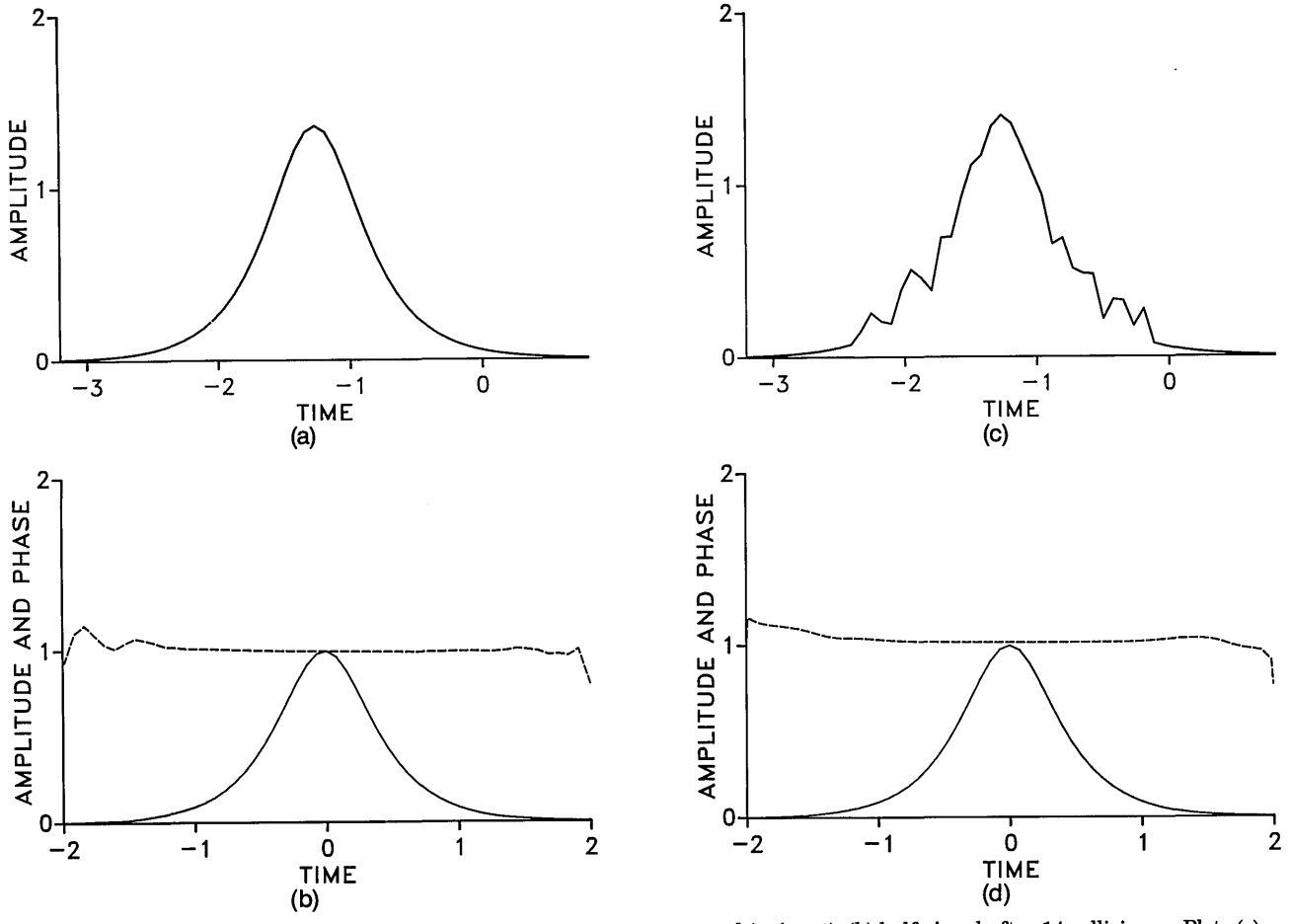

Fig. 7. Predicted pulse profiles after traversing a 14-section loop: (a) control (at input), (b) half-signal after 14 collisions. Plots (c) and (d) are the same as (a) and (b) but with noisy, degraded control. The solid curve is the amplitude. The dotted curve is the collision-induced phase in units of π radians.

We have demonstrated the solitary-wave collision principle experimentally. Our results will be published elsewhere.

Synchronizer

The same system can be used to correct timing errors (less than the intersymbol spacing) in incoming pulses. The signal pulse is generated locally and is thus a standard in terms of both shape and timing. The control pulse is the incoming pulse, which is likely to have suffered undesirable timing shifts. The key feature of the device is that the control is entirely replaced by the signal, regardless of timing shifts and background radiation in the control channel. The timing insensitivity is achieved through the use of fiber sections that are longer than the minimum required for a solitary-wave collision. Thus the collision can occur at any point along the fiber section.

Synchronization is important for the proposed long-distance transmission system.[12-14] The same device could be used to suppress the spontaneous noise generated in Raman or semiconductor amplifiers.[15-18]

XOR Gate with Fan-Out

The same loop can be used as a regenerative XOR gate with fan-out if a polarization-sensitive coupler, which cross-couples 100% of pulse B but 0% of orthogonally polarized light, is added to the output port outside the loop, as is shown in Fig. 8. A polarizer is no longer necessary. We remind the reader that the polarization-sensitive coupler that closes the loop splits the C pulse 50/50 but is 100/0 or (0/100) for A and B. Consider A and B as the inputs, which, if present, arrive at the loop at approximately the same time. Note that A and B will be counterpropagating within the loop. C is generated at each clock cycle and is reflected by the loop in the absence of other pulses. If either A or B, but not both, is present, half of C acquires a π phase shift, and the reconstructed C is transmitted at the coupler. If both A and B are present, both halves of C are phase shifted, and C is reflected.

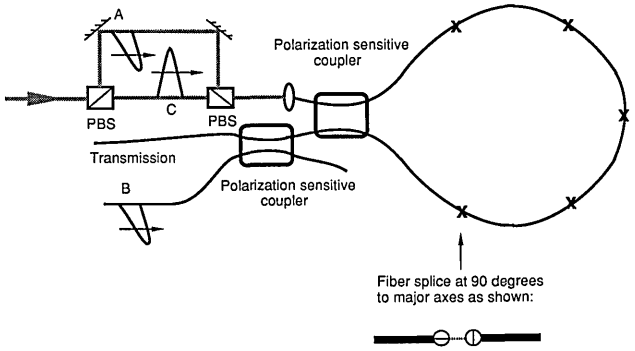

Fig. 8. Simple ring interferometer XOR gate configuration. The gate is regenerative and has fan-out.

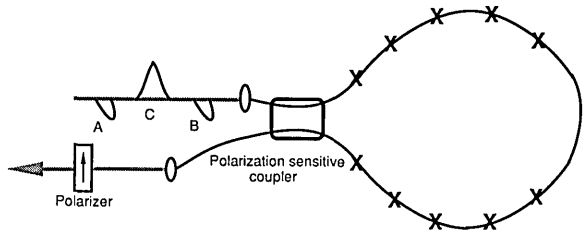

Fig. 9. Alternative XOR gate configuration. Note that both the signal and control pulses enter through the same input port.

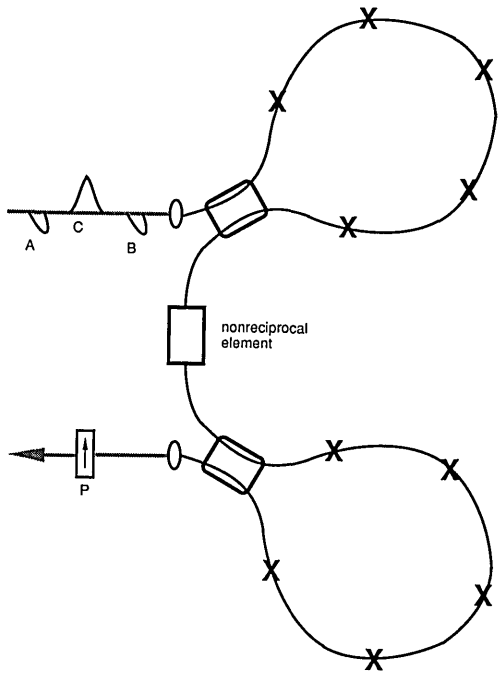

Fig. 10. Proposed regenerative AND gate with fan-out, utilizing solitary-wave collisions. Two loops (cf. Fig. 5) are in series, with a nonreciprocal element between the loops. A and B are the incoming pulses, while C is a locally generated higher-intensity pulse.

The extra polarization-selective coupler can be eliminated by doubling the length of the loop and reintroducing a polarizer (Fig. 9). Half of the loop is reserved for C–A collisions, while the other half is for C–B collisions.

AND Gate with Fan-Out

We can construct a superior AND gate by simply placing two loops in series, with a nonreciprocal element between the loops, as is shown in Fig. 10. The couplers are 50/50 for pulse C and 100/0 for A and B. Therefore each loop is reflective for C in the absence of other pulses. The fiber sections in the first loop are selected so that C interacts with A only. In the presence of A, half of C picks up a π phase shift in the first loop, and, on recombination, C is transmitted through the first loop. The fiber sections in the second loop are chosen so that C and B interact. The ordering of the fiber sections is simply reversed from that in the first loop. In the presence of B, C is transmitted through the second loop. A polarizer is placed at the output of the second loop in order to remove A and B. When A is present and B is absent, the nonreciprocal element allows C to escape from the cavity formed by the two loops.

The device has the desirable feature of being regenerative in the sense that the (possibly degraded and/or time-shifted) input pulses are replaced (if A and B are both present) by the control pulse. For this and the other devices, shape changes for pulses with area $>\pi/2$ do not dramatically affect the switching properties. The device provides a fan-out of 2 if C has twice the fundamental soliton power. In this case, we have an extremely favorable situation in that only first-order solitonlike pulses propagate within the gate. The section of fiber connecting the two loops can be extremely short ($\ll z_0$), so that C will not undergo any significant shape change between loops. Operating entirely with $N = 1$ solitons implies that the soliton period need not be much longer than each loop in order to avoid pulse reshaping within the loops.

CONCLUSION

We proposed a new design of a nonlinear fiber loop intensity switch. We also discussed switching devices and a synchronizer or timing drift corrector, employing a multiple solitary-wave collision scheme. Regenerative AND and XOR gates (together, a complete Boolean system) with fan-out are proposed. Predicted pulse distortion is small in all designs. None of these devices relies on critical input pulse timing.

ACKNOWLEDGMENTS

The support of National Science Foundation grant EET 8703404 and Joint Services Electronics Program contract DAAL03-89-C-0001 is gratefully acknowledged. Portions of this research were conducted using the Cornell National Supercomputer Facility, a resource of the Center for Theory and Simulations in Science and Engineering (Cornell Theory Center), which receives major funding from the National Science Foundation and IBM Corporation, with additional support from New York State and members of the Corporate Research Institute. J. D. Moores is grateful to the U.S. Office of Naval Research and to the Research Laboratory of Electronics at MIT for fellowship support. The authors thank undergraduate Farzana I. Khatri for her helpful graphics software support.

REFERENCES

1. A. Lattes, H. A. Haus, F. J. Leonberger, and E. P. Ippen, IEEE J. Quantum Electron. **QE-19,** 1718–1723 (1983).
2. K. Otsuka, Opt. Lett. **8,** 471–473 (1988).
3. N. J. Doran, D. S. Forrester, and B. K. Nayar, Electron. Lett. **25,** 267–269 (1989).
4. N. J. Doran and D. Wood, Opt. Lett. **13,** 56–58 (1988).
5. K. J. Blow, N. J. Doran, and B. K. Nayar, Opt. Lett. **14,** 754–757 (1989).
6. M. N. Islam, E. R. Sunderman, R. H. Stolen, W. Pleibel, and J. R. Simpson, Opt. Lett. **14,** 811–813 (1989).
7. C. R. Menyuk, J. Opt. Soc. Am. B **5,** 392–402 (1988).
8. T. R. Taha and M. J. Ablowitz, J. Comput. Phys. **55,** 203–215 (1984).
9. N. J. Doran, K. J. Blow, and D. Wood, Proc. Soc. Photo-Opt. Instrum. Eng. **836,** 238–243 (1987).
10. L. Mollenauer, R. Stolen, and J. Gordon, Phys. Rev. Lett. **45,** 1095–1098 (1980).

11. K. Suzuki and M. Nakazawa, Electron. Lett. (to be published).
12. A. Hasegawa, Opt. Lett. **8,** 650–652 (1983).
13. L. F. Mollenauer, R. H. Stolen, and M. N. Islam, Opt. Lett. **10,** 229–231 (1985).
14. L. F. Mollenauer and K. Smith, Opt. Lett. **13,** 675–677 (1988).
15. Y. Aoki, IEEE J. Lightwave Technol. **6,** 1225–1239 (1988).
16. M. J. O'Mahony, IEEE J. Lightwave Technol. **6,** 531–544 (1988).
17. T. Saitoh and T. Mukai, IEEE J. Lightwave Technol. **6,** 1656–1664 (1988).
18. J. P. Gordon and H. A. Haus, Opt. Lett. **11,** 665–667 (1986).